Published in final edited form as:
Brain Res. 2006 August 9; 1104(1): 45–54. doi:10.1016/j.brainres.2006.05.067.

BDNF enhances dendritic Ca^{2+} signals evoked by coincident EPSPs and back-propagating action potentials in CA1 pyramidal neurons

Lucas Pozzo-Miller*
Department of Neurobiology and Civitan International Research Center, University of Alabama at Birmingham, 1825 University Blvd. Birmingham, AL 35294-2182, Alabama, USA

Abstract

BDNF, a member of the neurotrophin family, is emerging as a key modulator of synaptic structure and function in the CNS. Due to the critical role of postsynaptic Ca^{2+} signals in dendritic development and synaptic plasticity, we tested whether long-term exposure to BDNF affects Ca^{2+} elevations evoked by coincident excitatory postsynaptic potentials (EPSPs) and back-propagating action potentials (bAPs) in spiny dendrites of CA1 pyramidal neurons within hippocampal slice cultures. In control neurons, a train of 5 coincident EPSPs and bAPs evoked Ca^{2+} elevations in oblique radial branches of the main apical dendrite that were of similar amplitude than those evoked by a train of 5 bAPs alone. On the other hand, dendritic Ca^{2+} signals evoked by coincident EPSPs and bAPs were always larger than those triggered by bAPs in CA1 neurons exposed to BDNF for 48 h. This difference was not observed after blockade of NMDA receptors (NMDARs) with D,L-APV, but only in BDNF-treated neurons, suggesting that Ca^{2+} signals in oblique radial dendrites include a synaptic NMDAR-dependent component. Co-treatment with the receptor tyrosine kinase inhibitor k-252a prevented the effect of BDNF on coincident dendritic Ca^{2+} signals, suggesting the involvement of neurotrophin Trk receptors. These results indicate that long-term exposure to BDNF enhances Ca^{2+} signaling during coincident pre- and postsynaptic activity in small spiny dendrites of CA1 pyramidal neurons, representing a potential functional consequence of neurotrophin-mediated dendritic remodeling in developing neurons.

Keywords

BDNF; Ca^{2+} imaging; CA1; Hippocampus; NMDA receptor; Pyramidal neuron; Synapse; TrkB

1. Introduction

Different models of activity-dependent synaptic development and plasticity postulate the existence of extracellular signaling molecules that enhance or stabilize synchronously active synapses. Neurotrophins have been postulated to play such role because their synthesis and release are regulated by neuronal activity, they activate prominent signaling pathways in neurons, and they are necessary for dendritic development and long-term changes in synaptic strength (McAllister et al., 1999; Poo, 2001; Tyler et al., 2002a; Bramham and Messaoudi, 2005). Because the spatiotemporal pattern of transient Ca^{2+} elevations is fundamental for neuronal development and synaptic plasticity (Zucker, 1999; Spitzer et al., 2004), their

*Fax: +1 205 934 6571., lucaspm@uab.edu.

modulation represents a potential target for neurotrophin action (McCutchen et al., 2002; Amaral and Pozzo-Miller, 2005).

The extensive dendrites of central neurons are the principal sites for excitatory synaptic input mediated by ligand-gated receptors, in addition to expressing several voltage-gated conductances that endow them with active properties (Johnston et al., 1996). The ensuing complex interactions between afferent synaptic activity and intrinsic excitability in active dendrites make them substrate of substantial computational power (Hausser and Mel, 2003). During trains of action potentials, CA1 pyramidal neurons display widespread dendritic Ca^{2+} transients caused by Na^{+}-dependent back-propagating action potentials (bAPs) that in turn activate voltage-gated Ca^{2+} channels (Jaffe et al., 1992; Spruston et al., 1995). On the other hand, Ca^{2+} signals evoked by synaptic activation of NMDA receptors (NMDAR) in CA1 pyramidal neurons are initially restricted to dendritic spines (Petrozzino et al., 1995; Emptage et al., 1999; Mainen et al., 1999; Pozzo-Miller et al., 1999; Kovalchuk et al., 2000; Nimchinsky et al., 2004). Of relevance to associative models of synaptic plasticity, Ca^{2+} transients evoked by coincident excitatory postsynaptic potentials (EPSPs) and bAPs within individual spines of hippocampal and neocortical pyramidal neurons exhibit a supralinear relationship (Yuste and Denk, 1995; Koester and Sakmann, 1998; Nevian and Sakmann, 2004). Such supralinearity of spine Ca^{2+} signals is thought to originate from the simultaneous activation of NMDAR during the EPSP and the removal of their Mg^{2+} block by the back-propagating spike (Schiller et al., 1998). These features of highly branched, spiny dendrites with active conductances have been recently related to several rules of compartmentalized cellular excitability, dendritic integration, as well as synaptic and intrinsic plasticity (Goldberg and Yuste, 2005; Johnston et al., 2003; Polsky et al., 2004; Schaefer et al., 2003).

In the present report, we present evidence that long-term BDNF exposure enhances Ca^{2+} signals in spiny dendrites during coincident pre- and postsynaptic activity. In control CA1 pyramidal neurons, brief trains of paired EPSPs and bAPs evoked Ca^{2+} transients in oblique radial branches of the main apical dendrite that were similar to those evoked by bAPs alone. On the other hand, Ca^{2+} signals evoked by coincident EPSPs and bAPs were always larger than those triggered by bAPs in CA1 neurons exposed to BDNF. The NMDAR antagonist D,L-APV prevented this effect, indicating that either direct Ca^{2+} influx through synaptic NMDAR in spines, or voltage-gated influx through Ca^{2+} channels activated by the NMDAR-mediated depolarization contributes to dendritic Ca^{2+} elevations. Consistent with the activation of Trk receptors, coincubation with the receptor tyrosine kinase inhibitor k-252a prevented the effect of BDNF on dendritic Ca^{2+} signals evoked by coincident pre- and postsynaptic activity.

2. Results

The aim of this study was to examine whether long-term BDNF exposure modulates dendritic Ca^{2+} elevations evoked by coincident pre- and postsynaptic activity in CA1 pyramidal neurons maintained in hippocampal slice cultures (Fig. 1A). Slice cultures were kept in serum-free media as controls, exposed to BDNF for 48 h (250 ng/mL) in the absence and presence of the receptor tyrosine kinase inhibitor k-252a (200 nM) or exposed to k-252a alone (200 nM, 48 h). The Ca^{2+} indicators bis-fura-2 (250 μM) or OGB-1 (100 μM) were included in the whole-cell recording pipette, and simultaneous fluorescence imaging was restricted to secondary spiny dendrites after they branched from the main apical primary dendrite (50–100 μm from the soma; Fig. 1A). All data were obtained from a total of 39 CA1 pyramidal neurons. Neurons from all treatment groups had similar values of resting membrane potential (control-57 ± 2 mV, $n = 10$; BDNF-60 ± 1 mV, $n = 10$; BDNF + k252a-55 ± 1 mV, $n = 4$; k252a-54 ± 1 mV, $n = 4$; ANOVA $P > 0.05$). In addition, BDNF did not affect the resting Ca^{2+} concentration in these secondary spiny dendrites (control bisfura-2 357/380 nm ratio = 0.15 ± 0.02, $n = 4$; BDNF 0.14 ± 0.03, $n = 4$; *t* test $P > 0.05$).

Fig. 1A shows a montage of fluorescence images of a representative CA1 pyramidal neuron loaded with OGB-1 through the somatic whole-cell electrode. Measurements of Ca^{2+}-indicator fluorescence intensity were obtained from secondary spiny dendrites after branching from the main apical primary dendrite, which sometimes included the so-called radial oblique dendrites (Frick et al., 2003;Losonczy and Magee, 2006). Intracellular Ca^{2+} elevations were evoked by one of the following protocols (Fig. 1B): (i) a 20-Hz train of 5 subthreshold EPSPs (5–10 mV in amplitude each) evoked by afferent fiber stimulation with an extracellular electrode positioned parallel to the Schaeffer collaterals in CA1 *stratum radiatum*, always within 100 μm of *stratum pyramidale*, and within 20 μm of the dendrites of the dye-filled cell; (ii) a 20-Hz train of 5 back-propagating action potentials (bAPs) triggered by short (5 ms) depolarizing current pulses via the somatic recording electrode; (iii) a 20-Hz train of 5 coincident EPSPs and bAPs, where each bAP was triggered after a 10-ms delay from the extracellular afferent stimulation. Fig. 1C shows Ca^{2+} transients within the color-coded ROIs in Fig. 1A in response to a train of subthreshold EPSPs (left), a train of 5 bAPs (middle), or a train of 5 coincident EPSPs-bAPs (right). In all the experiments described here, the imaging was performed in the absence of BDNF or k-252a, which were present only in the culture media during 48 h in vitro, but not in the recording ACSF. Neurons that fired complex spikes, especially during coincident trains of EPSP-bAP, were discarded and not further studied to avoid the confounding effect of an additional source of voltage-dependent Ca^{2+} influx, i.e., regenerative Ca^{2+} spikes (Hoffman et al., 2002).

2.1. Dendritic Ca^{2+} signals evoked by coincident EPSP-bAP trains were larger than those evoked by bAPs alone, but only in BDNF-treated neurons

The amplitude of dendritic Ca^{2+} signals evoked by trains of 5 EPSPs, 5 bAPs, or 5 coincident EPSP-bAP pairings were not significantly different between BDNF-treated and control neurons (Table 1; ANOVA $P > 0.05$). We next wondered how much bigger were dendritic Ca^{2+} signals evoked by coincident EPSP-bAP trains compared to those triggered by bAPs alone. In other words, what was the contribution of the EPSPs to the coincident EPSP-bAP train in terms of Ca^{2+} signals in secondary apical dendrites. To this aim, the ratio of the amplitude of Ca^{2+} signals triggered by coincident EPSP-bAP trains to that evoked by the bAP train alone (EPSP-bAP/bAP ratio) was used to estimate the contribution of the synaptically originated component of the Ca^{2+} signal (or membrane depolarization) to dendritic Ca^{2+} elevations. We found that a 20-Hz train of 5 coincident EPSPs and bAPs evoked dendritic Ca^{2+} transients in control neurons that were similar to those evoked by bAPs alone (control EPSP-bAP/bAP ratio: 0.947 ± 0.015, $n = 10$; Fig. 2A and Fig. 4A); this pattern was observed in all 10 control neurons. In sharp contrast, dendritic Ca^{2+} transients evoked by EPSPs and bAPs in BDNF-treated neurons were larger than those evoked by a 20-Hz train of 5 bAPs alone (BDNF EPSP-bAP/bAP ratio: 1.102 ± 0.028, $n = 13$; Student's t test $P = 0.0002$ vs. control; Fig. 3A and Fig. 4A). In a separate set of experiments, essentially the same results were obtained in neurons filled with the Ca^{2+} indicator bis-fura-2 (BDNF EPSP-bAP/bAP ratio: 1.275 ± 0.147, $n = 4$; control EPSP-bAP/bAP ratio: 0.8712 ± 0.069, $n = 4$; t test $P < 0.05$).

2.2. The role of NMDARs in dendritic Ca^{2+} signals during coincident EPSP-bAP

To determine the role of NMDARs in dendritic Ca^{2+} signals evoked by coincident pre- and postsynaptic activity, we first confirmed that dendritic Ca^{2+} elevations evoked by a train of 5 subthreshold EPSPs alone were significantly reduced by the competitive NMDAR antagonist D,L-APV (100 μM; BDNF cells: 76 ± 8% inhibition, $n = 8$; control cells: 66 ± 7% inhibition, $n = 9$; paired t test $P < 0.05$; Fig. 2B and Fig. 3B). Next, we tested whether synaptically activated NMDARs contribute to the observed coincident dendritic Ca^{2+} signals. Indeed, D,L-APV caused a small but significant reduction in dendritic Ca^{2+} signals evoked by coincident EPSP-bAP pairings in both BDNF-treated (20 ± 2% inhibition, $n = 8$), and control cells (24 ± 5% inhibition, $n = 9$; paired t test $P < 0.05$; Fig. 2B and Fig. 3B). In addition, the EPSP-bAP/bAP

ratio was reduced by D,L-APV in BDNF-treated neurons (BDNF EPSP-bAP/bAP ratio after D,L-APV: 1.009 ± 0.044; vs. BDNF EPSP-bAP/bAP ratio: 1.11 ± 0.039, $n = 8$; paired t test $P = 0.0274$), making it comparable to those observed in untreated neurons (Fig. 4B). However, the EPSP-bAP/bAP ratio was not affected by D,L-APV in control untreated neurons (control EPSP-bAP/bAP ratio after D,L-APV: 0.9311 ± 0.015; vs. control EPSP-bAP/bAP ratio: 0.9411 ± 0.016, $n = 9$; paired t test $P = 0.3002$; Fig. 4B). From these observations, we interpret that either Ca^{2+} influx through synaptic NMDAR or through voltage-gated Ca^{2+} channels activated by the NMDAR-mediated depolarization contributes to dendritic Ca^{2+} elevations during coincident pre- and postsynaptic activity.

2.3. The role of Trk receptors in the BDNF effects on supralinear dendritic Ca^{2+} signals

The tyrosine kinase inhibitor k-252a was used to test whether the observed effect of BDNF was mediated through the activation of its Trk receptor. The inhibitor was applied together with BDNF or by itself at 200 nM, a concentration well established to specifically inhibit plasma membrane receptor tyrosine kinases, such as neurotrophin Trk receptors, and not soluble tyrosine kinases (Tapley et al., 1992). In addition, this concentration is effective in our system to prevent the BDNF-induced increase in docked vesicles, mEPSC frequency, and spine density in CA1 pyramidal neurons (Tyler and Pozzo-Miller, 2001). The EPSP-bAP/bAP ratio in neurons exposed to BDNF in the presence of k-252a was comparable to that of control cells (BDNF + k-252a EPSP-bAP/bAP ratio: 0.99 ± 0.015, $n = 4$; vs. BDNF EPSP-bAP/bAP ratio: 1.1 ± 0.029, $n = 13$; unpaired t test $P = 0.0045$; Fig. 4A). Similar to the actions of BDNF by itself, this inhibition was selective for the EPSP-bAP/bAP ratio, as k-252a did not affect the maximal amplitude of dendritic Ca^{2+} elevations evoked by trains of 5 subthreshold EPSPs, 5 bAPs, or 5 coincident EPSP-bAP pairings (Table 1; ANOVA $P > 0.05$). In addition, the EPSP-bAP/bAP ratio was not affected by D,L-APV in BDNF + k-252a cells (BDNF + k- 252a EPSP-bAP/bAP ratio after D,L-APV: 0.963 ± 0.013; vs. BDNF + k-252a EPSP-bAP/bAP ratio: 0.992 ± 0.015, $n = 4$; paired t test $P = 0.0755$; Fig. 4B). Lastly, application of k-252a by itself to control slices had no effect on any of these parameters (Table 1; ANOVA $P > 0.05$). Taken together, these results suggest that the effect of BDNF on coincident dendritic Ca^{2+} signals is mediated by Trk receptors.

3. Discussion

The present results show that, in CA1 pyramidal neurons exposed to BDNF, brief trains of coincident subthreshold EPSPs and bAPs evoke larger Ca^{2+} elevations in secondary branches of the main apical dendrites compared to those caused by bAP trains alone. This difference was not observed after NMDAR blockade, suggesting that either direct Ca^{2+} influx through synaptic NMDAR or voltage-gated influx through Ca^{2+} channels activated by the NMDAR-mediated depolarization contributes to dendritic Ca^{2+} elevations during coincident pre- and postsynaptic activity. Interestingly, this contribution was never observed in control untreated neurons. Consistent with the activation of Trk receptors, the receptor tyrosine kinase inhibitor k-252a prevented the effect of BDNF on coincident dendritic Ca^{2+} signals, making them comparable to those observed in control untreated neurons.

One of the best-characterized routes of Ca^{2+} entry relevant to synaptic plasticity are synaptically activated NMDARs located on dendritic spines (Connor et al., 1994; Yuste et al., 2000; Sabatini et al., 2001; Nimchinsky et al., 2002). A particular property of NMDARs, the voltage-dependent block by Mg^{2+}, enables them to detect coincident pre- and postsynaptic activity. This coincidence is translated into larger intracellular Ca^{2+} elevations when excitatory synaptic potentials are immediately followed by action potentials that back-propagate into synaptically innervated dendrites. By virtue of the synaptic activation of NMDARs, Ca^{2+} elevations within individual dendritic spines of hippocampal and neocortical pyramidal

neurons during coincident EPSP-bAP trains have been shown to be larger than the predicted algebraic sum of Ca^{2+} signals elicited by the subthreshold EPSP and bAP trains by themselves, i.e., they are supralinear (Yuste and Denk, 1995; Koester and Sakmann, 1998; Nevian and Sakmann, 2004). It is important to note that in the present manuscript we have not performed Ca^{2+} measurements within spine heads, but rather in secondary apical dendrites, known to be studded with spines (Müller and Connor, 1991; Harris et al., 1992; Petrozzino et al., 1995; Pozzo-Miller et al., 1999). In addition, we have not addressed whether dendritic Ca^{2+} signals evoked by different stimulation protocols have supra- or sublinear relationships, but rather calculated how much larger were the Ca^{2+} signals evoked by coincident EPSP-bAPs compared to those evoked by bAPs alone. This parameter is relevant to dendritic and synaptic function because pairing EPSPs with bAPs resulted in the amplification of dendritic action potentials and the resultant Ca^{2+} elevations, as well as potentiation of synaptic potentials (Magee and Johnston, 1997). It is important to note that our results do not contradict those of Magee and Johnston (Magee and Johnston, 1997), who found that pairing EPSPs with bAPs evoked larger Ca^{2+} elevations than bAP alone, for two reasons. First, Magee and Johnston (1997) imaged the main primary apical dendrite, whereas we have imaged the smaller radial branches off the main primary dendrite, recently dubbed “radial oblique dendrites” by the same authors (Frick et al., 2003; Losonczy and Magee, 2006). We focused on these secondary branches because they express a higher density of spines and of synaptic contacts than the main apical trunk, and because our prior work on BDNF-induced spine formation focused on these spiny secondary dendritic branches (Tyler and Pozzo-Miller, 2001, 2003; Alonso et al., 2004). These radial oblique dendrites have been shown to have different properties than the main apical trunk, including the amplitude of Ca^{2+} signals evoked by bAPs (Frick et al., 2003), and the generation of local dendritic spikes involving Na^{+}, Ca^{2+}, and K^{+} channels (Losonczy and Magee, 2006). Another potential reason for the difference with the Magee and Johnston (1997) observations is the fact that those studies were performed in acute hippocampal slices, whereas our measurements were done in organotypic slice cultures, a requirement for the long-term exposure to BDNF. Furthermore, our control slices have been kept in serum-free media to avoid the confounding effects of unknown growth factors in the equine serum, a consistently used and well-accepted control in neurotrophin studies in vitro. It is tempting to speculate that our serum-free neurons have impaired dendritic Ca^{2+} signaling compared to those from acutely prepared slices, and that BDNF rescued this impairment. Thus, our observation that only BDNF-treated neurons showed larger EPSP-bAP-evoked dendritic Ca^{2+} signals than bAP-driven signals suggests a potential mean by which BDNF participates in activity-dependent dendritic development and synaptic plasticity.

Accumulating evidence indicate that BDNF enhances NMDAR function in hippocampal neurons (Levine et al., 1998). Basal spiny dendrites of neocortical pyramidal neurons exhibit regenerative Ca^{2+} spikes mediated by NMDARs (Schiller et al., 2000), which could contribute to the observed Ca^{2+} signals during coincident EPSP-bAP trains described here [in addition to the recently described spikes in radial oblique dendrites of CA1 neurons by Losonczy and Magee (2006), see above]. In addition, BDNF rapidly enhances NMDA-induced currents in cultured hippocampal neurons, primarily through receptors containing NR2B subunits (Levine and Kolb, 2000). Thus, phosphorylation of NR1 and NR2B subunits by TrkB-initiated signaling cascades, as shown by Lin et al. (1998), is the most likely mechanism of immediate BDNF actions on NMDAR function. It is unclear at this time whether long-term BDNF exposure as studied here has similar effects on NMDARs. Because these effects on NMDARs occur within minutes of BDNF exposure it is unclear yet how they relate to the present observations. On the other hand, the effects of long-term BDNF exposure not only on spine density, but also on the geometry of individual spines (Tyler and Pozzo-Miller, 2001, 2003; Alonso et al., 2004), provide an alternative interpretation for the larger Ca^{2+} elevations in spiny dendrites evoked by coincident EPSPs and bAPs in BDNF-treated neurons. Indeed, recent computer simulations have shown that dendritic excitability, measured as the spatial spread of

spike back-propagation or spike threshold, is enhanced by increasing the density of dendritic spines, more so if spines are endowed with active conductances (Tsay and Yuste, 2002; Verzi et al., 2005).

The function of dendritic spines has been extensively investigated (Shepherd, 1996; Yuste and Bonhoeffer, 2001; Sabatini et al., 2001; Nimchinsky et al., 2002). Regarding their individual geometrical dimensions, recent studies have proposed that spine length in hippocampal pyramidal neurons contributes to spine-dendrite coupling of Ca^{2+} signals (Korkotian and Segal, 2000; Korkotian et al., 2004; Majewska et al., 2000). Furthermore, the dimensions and geometry of the spine neck in CA1 pyramidal neurons have been shown to determine NMDAR-dependent Ca^{2+} signaling in the parent dendrite (Noguchi et al., 2005). We interpret that the BDNF-induced structural remodeling of spiny dendrites has consequences for Ca^{2+} signals evoked by coincident pre- and postsynaptic activity. In this view, the increased spine density and the higher proportion of Type-I (stubby) spines observed in CA1 pyramidal neurons after BDNF exposure (Tyler and Pozzo-Miller, 2001, 2003; Alonso et al., 2004) contributes to spine-dendrite coupling of synaptic Ca^{2+} signals mediated by synaptic NMDRs. Consistent with this interpretation, synaptically initiated NMDA-dependent Ca^{2+} signals within spiny dendrites of CA1 pyramidal neurons are larger in hippocampal slice cultures exposed to estradiol, an observation that again correlates with the higher spine density of estradiol-treated neurons (Pozzo-Miller et al., 1999). It is worth noting that those larger Ca^{2+} signals in dendritic shafts in estrogen-treated neurons were evoked by afferent stimulation under voltage-clamp at depolarized potentials to evoke pharmacologically isolated NMDAR-mediated synaptic currents (Perkel et al., 1993; Malinow et al., 1994; Pozzo Miller et al., 1996), in contrast to the present observations that represent both voltage- and ligand-gated Ca^{2+} influx during bAPs alone, EPSPs alone, or coincident bAPs and subthreshold EPSPs. It is currently unknown whether estradiol promotes the formation of a morphologically specific spine type, as BDNF does (Tyler and Pozzo-Miller, 2003).

Considering that long and thin spines may isolate synaptically initiated spine Ca^{2+} transients from the parent dendrite and neighboring spines (Segal et al., 2000), and that synchronously coordinated dendritic and spine Ca^{2+} transients are critical for synaptic plasticity (Yuste and Bonhoeffer, 2001; Sabatini et al., 2001), BDNF may enhance synaptic plasticity not only by increasing spine density, but also the proportion of Type-I stubby spines. These larger spines with wider necks are thought to represent spines that acquired AMPA receptors immediately after the induction of long-term potentiation (Matsuzaki et al., 2001; Kasai et al., 2003), and thus enhance spine-dendrite coupling leading to widespread dendritic Ca^{2+} signaling during excitatory synaptic transmission (Noguchi et al., 2005). Together with the morphological effects of BDNF on presynaptic terminals (Tyler et al., 2002b) and postsynaptic spine growth and form (Tyler and Pozzo-Miller, 2001, 2003; Alonso et al., 2004), we propose that the larger Ca^{2+} signals in spiny dendrites during coincident pre- and postsynaptic activation represent a physiological consequence of the structural BDNF actions at hippocampal synapses. The combination of these structural and physiological effects in the hippocampus may underlie the role of BDNF in the consolidation of synaptic plasticity and hippocampal-dependent learning and memory (Tyler et al., 2002a; Bramham and Messaoudi, 2005).

4. Experimental procedures

4.1. Organotypic slice cultures and treatments

Hippocampal slices from postnatal day 7 Sprague–Dawley rats were cultured on interface tissue culture inserts (Millicell-CM, Millipore; Billerica, MA) inside a 36 °C, 5% CO_2, 98% relative humidity incubator, as described previously (Pozzo Miller et al., 1993Tyler and Pozzo-Miller, 2003). The concentration of equine serum in the medium was gradually reduced over a 48-h period starting at 4 days in vitro (div) (Tyler and Pozzo-Miller, 2001, 2003; Alonso et

al., 2004). In this manner, the potential confounding effects of other growth factors and hormones in the serum were eliminated by using a defined serum-free medium as a control (Neurobasal-A, plus B-27 supplement; Life Technologies, Gaithersburg, MD). Antibiotics, antimycotics, or proliferation inhibitors were never included in the culture media. All procedures were performed following national and international ethics guidelines and approved by the IACUC (UAB).

Following 24 h in serum-free media, 7 div slices (Fig. 1A) were treated with BDNF (250 ng/mL; provided by Amgen, Thousand Oaks, CA) for 48 h. This treatment regime was used in our previous studies of the effects of BDNF on synaptic structure and function (Tyler and Pozzo-Miller, 2001,2003;Alonso et al., 2004). The tyrosine kinase inhibitor k-252a (Calbiochem, La Jolla, CA) was applied together with BDNF or by itself at 200 nM, a concentration well established to specifically inhibit plasma membrane receptor tyrosine kinases and not soluble tyrosine kinases (Tapley et al., 1992).

4.2. Simultaneous whole-cell recording and Ca^{2+} imaging

Slice cultures were individually transferred to an immersion-type chamber perfused with artificial cerebrospinal fluid (ACSF) at room temperature, containing (in mM): 124 NaCl; 2 KCl; 1.3 $MgSO_4$; 1.24 KH_2PO_4; 17.6 $NaHCO_3$; 2.5 $CaCl_2$; 10 D-glucose; 310–320 mOsm; bubbled with 95% O_2/5% CO_2. Whole-cell recordings were performed with patch pipettes containing (in mM): 120 K-gluconate; 17.5 KCl; 10 NaCl; 4 Mg-ATP; 0.4 Na-GTP; 10 NaHEPES; 10 creatine phosphate; 280–290 mOsm; pH 7.2 (final resistance 4–6 MΩ). All reagents were from Sigma (St. Louis, MO). The hexapotassium salts of bis-fura-2 (250 μM) or Oregon-Green-BAPTA-1 (OGB-1; 100 μM; Molecular Probes, Eugene, OR) were included in the patch pipette and used as Ca^{2+} indicators.

CA1 pyramidal neurons were visualized with infrared-DIC optics in a fixed-stage upright microscope (Axioskop FS; Zeiss, Thornwoood, NY) using a water-immersion 63× objective (0.9 NA; Zeiss Achroplan; Fig. 1A) (Pozzo-Miller et al., 1999). Tight-seal whole-cell intracellular recordings were performed under current-clamp using an Axoclamp-2B amplifier (Axon Instruments, Foster City, CA), as described (Pozzo Miller et al., 1995). Electrical signals were filtered at 2 kHz and digitized at 10 kHz using an ITC-18 digitizing interface (Instrutech, Great Neck, NY). Afferent stimulation (100 μs square monopolar pulses) was performed with an extracellular patch pipette filled with aCSF and positioned parallel to the Schaeffer collaterals in CA1 *stratum radiatum*, always within 100 μm of *stratum pyramidale*, and within 20 μm of the dendrites of the dye-filled cell, using a TTL-driven constant-current stimulator (ISO-Flex, AMPI, Jerusalem, Israel). Simultaneous digital imaging was performed after 15–20 min from whole-cell access to allow for dye equilibration (Fig. 1A) (Pozzo Miller et al., 1996;McCutchen et al., 2002). Bis-fura-2 was excited at 357 nm and 380 nm and OGB-1 at 488 nm using a monochromator (12 nm band width; Polychrome IV, TILL Photonics, Planegg, Germany). Fluorescence emission of bis-fura-2 (510 nm) and OGB-1 (515 nm) was reflected and filtered with matching dichroic mirrors and emission filter sets (Chroma Technology, Brattleboro, VT). Digital images were acquired with a cooled CCD camera with a frame-transfer back-illuminated sensor (Quantix EEV57; Photometrics, Tucson, AZ). CCD subarrays of ~100 by ~200 pixels were read-out in ~10 ms using 3 × 1 on-chip pixel binning. This read-out speed allowed frame rates of ~20–33 frames per second when using exposure times 20–40 ms per frame. Custom-written software was used to perform synchronized electrical and optical recordings with control of the amplifier, stimulator, and mono-chromator (courtesy of Dr. Takafumi Inoue, The University of Tokyo, Japan), as described (Pozzo-Miller et al., 1999).

Intracellular Ca^{2+} concentration was estimated from bisfura-2 fluorescence images using the isosbestic method (Neher and Augustine, 1992). Image frames at 357 nm excitation (Ca^{2+}-insensitive wavelength calibrated in our system) were acquired before and after a continuous

sequence of 380 nm excitation frames to generate pixel-by-pixel ratio images and time course plots. Peak Ca^{2+} levels were calculated by subtracting basal pre-stimulus 357/380 nm ratios (R_0, averaged from at least four frames) from the 357/380 nm ratio at the peak of the response (Rp), and referred to as $\Delta R = R_p - R_0$. For experiments using OGB-1, free Ca^{2+} concentration levels were estimated from relative fluorescence intensity changes, and expressed as % $\Delta F/F_0$, a reliable estimator provided that Ca^{2+} elevations do not saturate the dye (Maravall et al., 2000). None of the protocols used in the present studies, i.e., trains of 5 subthreshold EPSPs, 5 bAPs, or 5 coincident EPSP-bAP, seemed to saturate OGB-1 (K_d ~200 nM) or bis-fura-2 (K_d ~370 nM) because stronger stimulation (i.e., trains of 10–20 bAPs) evoked $\Delta F/F_0$ signals that increased linearly in amplitude (data not shown) (Maravall et al., 2000). Basal pre-stimulus fluorescence intensity (F0) was obtained by averaging fluorescence intensity for least four image frames before stimulus delivery. Fluorescence intensities were measured within ROIs (~10 by ~10 pixels) on small diameter secondary spiny dendrites, and over a region over the slice but outside of the dye-filled neuron used for background subtraction. To avoid excessive dye photobleaching and cellular phototoxicity, exposure to excitation light was limited to <2 s during the acquisition of image sequences (20–30 frames). Bleaching of indicator dyes was less than 5% during these short movies and thus was not corrected.

All data are expressed as the mean ± standard error of the mean (SEM). Statistical differences were assessed by paired and unpaired Student's *t* tests, or ANOVA followed by Tukey's multiple comparisons test as post hoc test, all using Prism (GraphPad, San Diego, CA); $P < 0.05$ was considered significant.

Acknowledgments

I would like to thank Rodolfo Llinás (NYU), John Hablitz (UAB), and Robin Lester (UAB) for helpful discussions and comments on the manuscript, Takafumi Inoue (University of Tokyo) for continuous support of the acquisition and analysis software, William J Tyler (Harvard University) for initial image analyses, Antonio Campos-Torres for the NeuN immunostaining of Fig. 1A, and Michelle Amaral for preparation and maintenance of organotypic slice cultures.

This study was supported by NIH grants RO1-NS40593 (LP-M), MRRC P30-HD38985, and PO1-HD38760, Civitan International Foundation, and AMGEN for the supply of BDNF. LP-M is a McNulty Civitan Scientist.

REFERENCES

Alonso M, Medina JH, Pozzo-Miller L. ERK1/2 activation is necessary for BDNF to increase dendritic spine density in hippocampal CA1 pyramidal neurons. Learn. Mem 2004;11:172–178. [PubMed: 15054132]

Amaral, MD.; Pozzo-Miller, L. On the role of neurotrophins in dendritic calcium signaling: implications for hippocampal transsynaptic plasticity. In: Stanton, PK.; Bramham, CR.; Scharfman, HE., editors. Synaptic Plasticity and Transsynaptic Signaling. New York: Springer Science and Business Media; 2005.

Bramham CR, Messaoudi E. BDNF function in adult synaptic plasticity: the synaptic consolidation hypothesis. Prog. Neurobiol 2005;76:99–125. [PubMed: 16099088]

Connor JA, Pozzo Miller LD, Petrozzino J, Muller W. Calcium signaling in dendritic spines of hippocampal neurons. J. Neurobiol 1994;25:234–242. [PubMed: 8195788]

Emptage N, Bliss TV, Fine A. Single synaptic events evoke NMDA receptor-mediated release of calcium from internal stores in hippocampal dendritic spines. Neuron 1999;22:115–124. [PubMed: 10027294]

Frick A, Magee J, Koester HJ, Migliore M, Johnston D. Normalization of Ca^{2+} signals by small oblique dendrites of CA1 pyramidal neurons. J. Neurosci 2003;23:3243–3250. [PubMed: 12716931]

Goldberg JH, Yuste R. Space matters: local and global dendritic Ca^{2+} compartmentalization in cortical interneurons. Trends. Neurosci 2005;28:158–167. [PubMed: 15749170]

Harris KM, Jensen FE, Tsao B. Three-dimensional structure of dendritic spines and synapses in rat hippocampus (CA1) at postnatal day 15 and adult ages: implications for the maturation of synaptic physiology and long-term potentiation. J. Neurosci 1992;12:2685–2705. [PubMed: 1613552]

Hausser M, Mel B. Dendrites: bug or feature? Curr. Opin. Neurobiol 2003;13:372–383. [PubMed: 12850223]

Hoffman DA, Sprengel R, Sakmann B. Molecular dissection of hippocampal theta-burst pairing potentiation. Proc. Natl. Acad. Sci. U. S. A 2002;99:7740–7745. [PubMed: 12032353]

Jaffe DB, Johnston D, Lasser-Ross N, Lisman JE, Miyakawa H, Ross WN. The spread of Na^+ spikes determines the pattern of dendritic Ca^{2+} entry into hippocampal neurons. Nature 1992;357:244–246. [PubMed: 1350327]

Johnston D, Magee JC, Colbert CM, Cristie BR. Active properties of neuronal dendrites. Annu. Rev. Neurosci 1996;19:165–186. [PubMed: 8833440]

Johnston D, Christie BR, Frick A, Gray R, Hoffman DA, Schexnayder LK, Watanabe S, Yuan LL. Active dendrites, potassium channels and synaptic plasticity. Philos. Trans. R. Soc. Lond., B Biol. Sci 2003;358:667–674. [PubMed: 12740112]

Kasai H, Matsuzaki M, Noguchi J, Yasumatsu N, Nakahara H. Structure–stability–function relationships of dendritic spines. Trends. Neurosci 2003;26:360–368. [PubMed: 12850432]

Koester HJ, Sakmann B. Calcium dynamics in single spines during coincident pre-and postsynaptic activity depend on relative timing of back-propagating action potentials and subthreshold excitatory postsynaptic potentials. Proc. Natl. Acad. Sci. U. S. A 1998;95:9596–9601. [PubMed: 9689126]

Korkotian E, Segal M. Structure–function relations in dendritic spines: is size important? Hippocampus 2000;10:587–595. [PubMed: 11075829]

Korkotian E, Holcman D, Segal M. Dynamic regulation of spine-dendrite coupling in cultured hippocampal neurons. Eur J. Neurosci 2004;20:2649–2663. [PubMed: 15548208]

Kovalchuk Y, Eilers J, Lisman J, Konnerth A. NMDA receptor-mediated subthreshold Ca^{2+} signals in spines of hippocampal neurons. J. Neurosci 2000;20:1791–1799. [PubMed: 10684880]

Levine ES, Kolb JE. Brain-derived neurotrophic factor increases activity of NR2B-containing *N*-methyl-d-aspartate receptors in excised patches from hippocampal neurons. J. Neurosci. Res 2000;62:357–362. [PubMed: 11054804]

Levine ES, Crozier RA, Black IB, Plummer MR. Brain-derived neurotrophic factor modulates hippocampal synaptic transmission by increasing *N*-methyl-d-aspartic acid receptor activity. Proc. Natl. Acad. Sci. U. S. A 1998;95:10235–10239. [PubMed: 9707630]

Lin SY, Wu K, Levine ES, Mount HT, Suen PC, Black IB. BDNF acutely increases tyrosine phosphorylation of the NMDA receptor subunit 2B in cortical and hippocampal postsynaptic densities. Brain Res. Mol. Brain Res 1998;55:20–27. [PubMed: 9645956]

Losonczy A, Magee JC. Integrative properties of radial oblique dendrites in hippocampal CA1 pyramidal neurons. Neuron 2006;50:291–307. [PubMed: 16630839]

Magee JC, Johnston D. A synaptically controlled, associative signal for Hebbian plasticity in hippocampal neurons. Science 1997;275:209–213. [PubMed: 8985013]

Mainen ZF, Malinow R, Svoboda K. Synaptic calcium transients in single spines indicate that NMDA receptors are not saturated. Nature 1999;399:151–155. [PubMed: 10335844]

Majewska A, Brown E, Ross J, Yuste R. Mechanisms of calcium decay kinetics in hippocampal spines: role of spine calcium pumps and calcium diffusion through the spine neck in biochemical compartmentalization. J. Neurosci 2000;20:1722–1734. [PubMed: 10684874]

Malinow R, Otmakhov N, Blum KI, Lisman J. Visualizing hippocampal synaptic function by optical detection of Ca^{2+} entry through the *N*-methyl-d-aspartate channel. Proc. Natl. Acad. Sci. U. S. A 1994;91:8170–8174. [PubMed: 7914703]

Maravall M, Mainen ZF, Sabatini BL, Svoboda K. Estimating intracellular calcium concentrations and buffering without wavelength ratioing. Biophys. J 2000;78:2655–2667. [PubMed: 10777761]

Matsuzaki M, Ellis-Davies GC, Nemoto T, Miyashita Y, Iino M, Kasai H. Dendritic spine geometry is critical for AMPA receptor expression in hippocampal CA1 pyramidal neurons. Nat. Neurosci 2001;4:1086–1092. [PubMed: 11687814]

McAllister AK, Katz LC, Lo DC. Neurotrophins and synaptic plasticity. Ann. Rev. Neurosci 1999;22:295–818. [PubMed: 10202541]

McCutchen ME, Bramham CR, Pozzo-Miller LD. Modulation of neuronal calcium signaling by neurotrophic factors. Int. J. Dev. Neurosci 2002;20:199–207. [PubMed: 12175855]

Müller W, Connor JA. Dendritic spines as individual neuronal compartments for synaptic Ca^{2+} responses. Nature 1991;354:73–76. [PubMed: 1682815]

Neher E, Augustine GJ. Calcium gradients and buffers in bovine chromaffin cells. J. Physiol 1992;450:273–301. [PubMed: 1331424]

Nevian T, Sakmann B. Single spine Ca^{2+} signals evoked by coincident EPSPs and backpropagating action potentials in spiny stellate cells of layer 4 in the juvenile rat somatosensory barrel cortex. J. Neurosci 2004;24:1689–1699. [PubMed: 14973235]

Nimchinsky EA, Sabatini BL, Svoboda K. Structure and function of dendritic spines. Annu. Rev. Physiol 2002;64:313–353. [PubMed: 11826272]

Nimchinsky EA, Yasuda R, Oertner TG, Svoboda K. The number of glutamate receptors opened by synaptic stimulation in single hippocampal spines. J. Neurosci 2004;24:2054–2064. [PubMed: 14985448]

Noguchi J, Matsuzaki M, Ellis-Davies GC, Kasai H. Spine-neck geometry determines NMDA receptor-dependent Ca^{2+} signaling in dendrites. Neuron 2005;46:609–622. [PubMed: 15944129]

Perkel DJ, Petrozzino JJ, Nicoll RA, Connor JA. The role of Ca^{2+} entry via synaptically activated NMDA receptors in the induction of long-term potentiation. Neuron 1993;11:817–823. [PubMed: 7902109]

Petrozzino JJ, Pozzo Miller LD, Connor JA. Micromolar Ca^{2+} transients in dendritic spines of hippocampal pyramidal neurons in brain slice. Neuron 1995;14:1223–1231. [PubMed: 7605633]

Polsky A, Mel BW, Schiller J. Computational subunits in thin dendrites of pyramidal cells. Nat. Neurosci 2004;7:621–627. [PubMed: 15156147]

Poo MM. Neurotrophins as synaptic modulators. Nat. Rev., Neurosci 2001;2:24–32. [PubMed: 11253356]

Pozzo Miller LD, Petrozzino JJ, Mahanty NK, Connor JA. Optical imaging of cytosolic calcium, electrophysiology, and ultrastructure in pyramidal neurons of organotypic slice cultures from rat hippocampus. NeuroImage 1993;1:109–120. [PubMed: 9343562]

Pozzo Miller LD, Petrozzino JJ, Connor JA. G protein-coupled receptors mediate a fast excitatory postsynaptic current in CA3 pyramidal neurons in hippocampal slices. J. Neurosci 1995;15:8320–8330. [PubMed: 8613765]

Pozzo Miller LD, Petrozzino JJ, Golarai G, Connor JA. Ca^{2+} release from intracellular stores induced by afferent stimulation of CA3 pyramidal neurons in hippocampal slices. J. Neurophysiol 1996;76:554–562. [PubMed: 8836243]

Pozzo-Miller LD, Inoue T, Murphy DD. Estradiol increases spine density and NMDA-dependent Ca^{2+} transients in spines of CA1 pyramidal neurons from hippocampal slices. J. Neurophysiol 1999;81:1404–1411. [PubMed: 10085365]

Sabatini BL, Maravall M, Svoboda K. Ca^{2+} signaling in dendritic spines. Curr. Opin. Neurobiol 2001;11:349–356. [PubMed: 11399434]

Schaefer AT, Larkum ME, Sakmann B, Roth A. Coincidence detection in pyramidal neurons is tuned by their dendritic branching pattern. J. Neurophysiol 2003;89:3143–3154. [PubMed: 12612010]

Schiller J, Schiller Y, Clapham DE. NMDA receptors amplify calcium influx into dendritic spines during associative pre- and postsynaptic activation. Nat. Neurosci 1998;1:114–118. [PubMed: 10195125]

Schiller J, Major G, Koester HJ, Schiller Y. NMDA spikes in basal dendrites of cortical pyramidal neurons. Nature 2000;404:285–289. [PubMed: 10749211]

Segal I, Korkotian I, Murphy DD. Dendritic spine formation and pruning: common cellular mechanisms? Trends Neurosci 2000;23:53–57. [PubMed: 10652540]

Shepherd GM. The dendritic spine: a multifunctional integrative unit. J. Neurophysiol 1996;75:2197–2210. [PubMed: 8793734]

Spitzer NC, Root CM, Borodinsky LN. Orchestrating neuronal differentiation: patterns of Ca^{2+} spikes specify transmitter choice. Trends Neurosci 2004;27:415–421. [PubMed: 15219741]

Spruston N, Schiller Y, Stuart G, Sakmann B. Activity-dependent action potential invasion and calcium influx into hippocampal CA1 dendrites. Science 1995;268:297–300. [PubMed: 7716524]

Tapley P, Lamballe F, Barbacid M. K252a is a selective inhibitor of the tyrosine protein kinase activity of the trk family of oncogenes and neurotrophin receptors. Oncogene 1992;7:371–381. [PubMed: 1312698]

Tsay D, Yuste R. Role of dendritic spines in action potential backpropagation: a numerical simulation study. J. Neurophysiol 2002;88:2834–2845. [PubMed: 12424316]

Tyler WJ, Pozzo-Miller LD. BDNF enhances quantal neurotransmitter release and increases the number of docked vesicles at the active zones of hippocampal excitatory synapses. J. Neurosci 2001;21:4249–4258. [PubMed: 11404410]

Tyler WJ, Pozzo-Miller L. Miniature synaptic transmission and BDNF modulate dendritic spine growth and form in rat CA1 neurones. J. Physiol 2003;553:497–509. [PubMed: 14500767]

Tyler WJ, Alonso M, Bramham CR, Pozzo-Miller LD. From acquisition to consolidation: on the role of brain-derived neurotrophic factor signaling in hippocampal-dependent learning. Learn. Mem 2002a; 9:224–237. [PubMed: 12359832]

Tyler WJ, Perrett SP, Pozzo-Miller LD. The role of neurotrophins in neurotransmitter release. Neuroscientist 2002b;8:524–531. [PubMed: 12467374]

Verzi DW, Rheuben MB, Baer SM. Impact of time-dependent changes in spine density and spine shape on the input–output properties of a dendritic branch: a computational study. J. Neurophysiol 2005;93:2073–2089. [PubMed: 15590735]

Yuste R, Bonhoeffer T. Morphological changes in dendritic spines associated with long-term synaptic plasticity. Annu. Rev. Neurosci 2001;24:1071–1089. [PubMed: 11520928]

Yuste R, Denk W. Dendritic spines as basic functional units of neuronal integration. Nature 1995;375:682–684. [PubMed: 7791901]

Yuste R, Majewska A, Holthoff K. From form to function: calcium compartmentalization in dendritic spines. Nat. Neurosci 2000;3:653–659. [PubMed: 10862697]

Zucker RS. Calcium- and activity-dependent synaptic plasticity. Curr. Opin. Neurobiol 1999;9:305–313. [PubMed: 10395573]

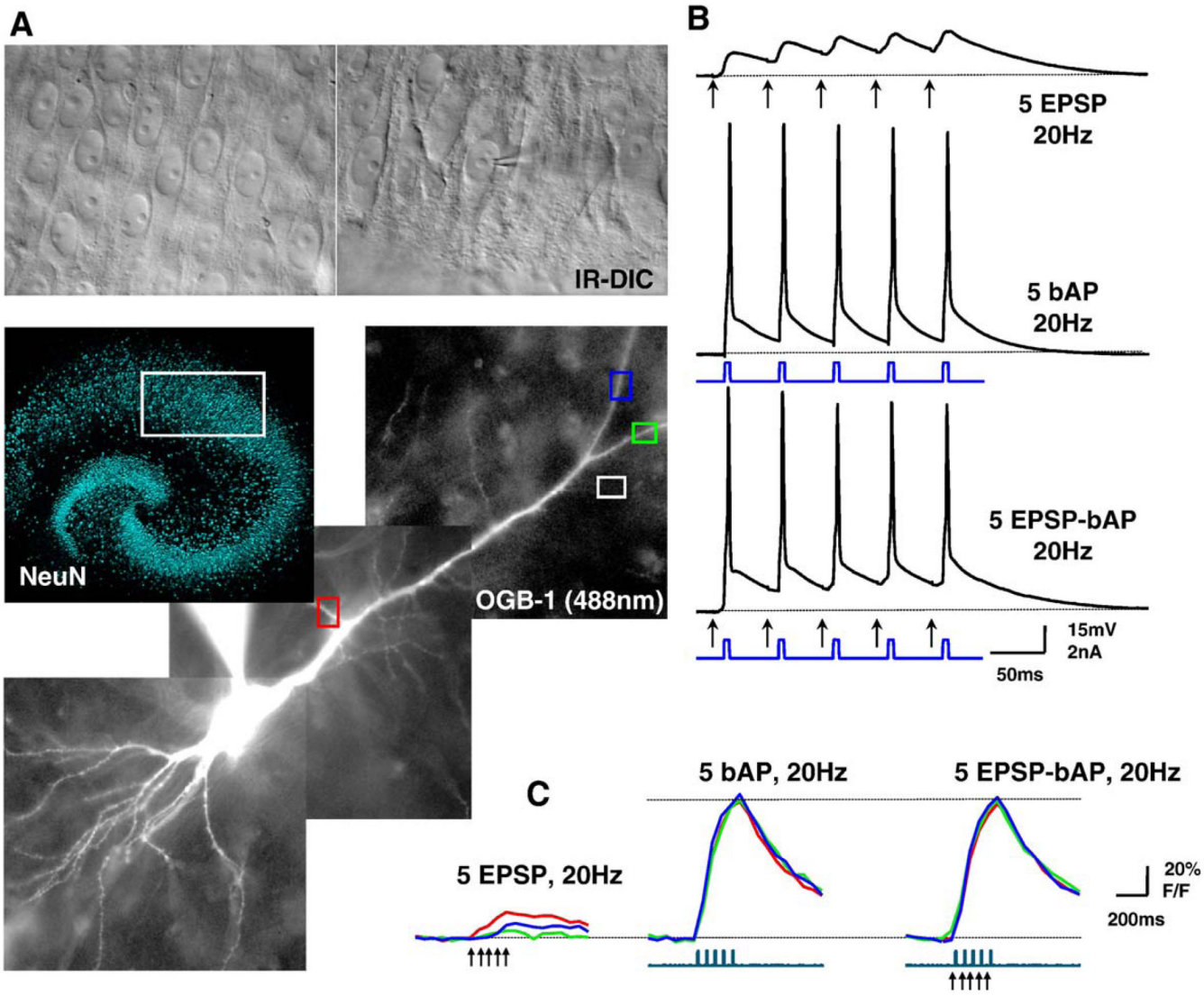

Fig. 1.

Dendritic Ca^{2+} changes evoked by trains of EPSPs, bAPs, or coincident EPSPs-bAPs in CA1 pyramidal neurons of hippocampal slice cultures. (A) Top, IR-DIC image of the CA1 region of a hippocampal slice culture. A whole-cell electrode is patched on a pyramidal neuron. Middle, low magnification image of a slice culture immunostained using NeuN antibody. NeuN immunofluorescence was performed as described (Alonso et al., 2004). The white box denotes the CA1 region used for whole-cell recording and imaging. Bottom, Montage of 3 different images of a CA1 neuron filled with the Ca^{2+} indicator dye Oregon-Green-BAPTA-1 (OGB-1) through the whole-cell recording electrode. Color-coded ROIs show secondary spiny dendrites where $\Delta F/F$ measurements were calculated (shown in panel C); the white ROI denotes a region over the slice and outside the dye-loaded cell for background subtraction. (B) Temporal relationship of subthreshold EPSPs evoked by extracellular afferent stimulation (arrows), and of bAPs elicited by direct current injection through the somatic recording electrode. Top trace shows a train of 5 EPSPs, middle trace shows a train of 5 bAPs, and bottom trace shows the a train of 5 EPSP-bAP pairings, all at 20 Hz. (C) Simultaneous current-clamp and Ca^{2+} imaging. The top traces represent the Ca^{2+} levels estimated by changes in OGB-1 fluorescence within the color-coded ROIs shown in panel A, expressed as % $\Delta F/F$, which is proportional to Ca^{2+}

concentration. The bottom traces represent membrane current. Arrowheads mark afferent stimulation. All data in panels B and C are from a sequential recording from the same CA1 pyramidal neuron. (For interpretation of the references to colour in this figure legend, the reader is referred to the web version of this article.)

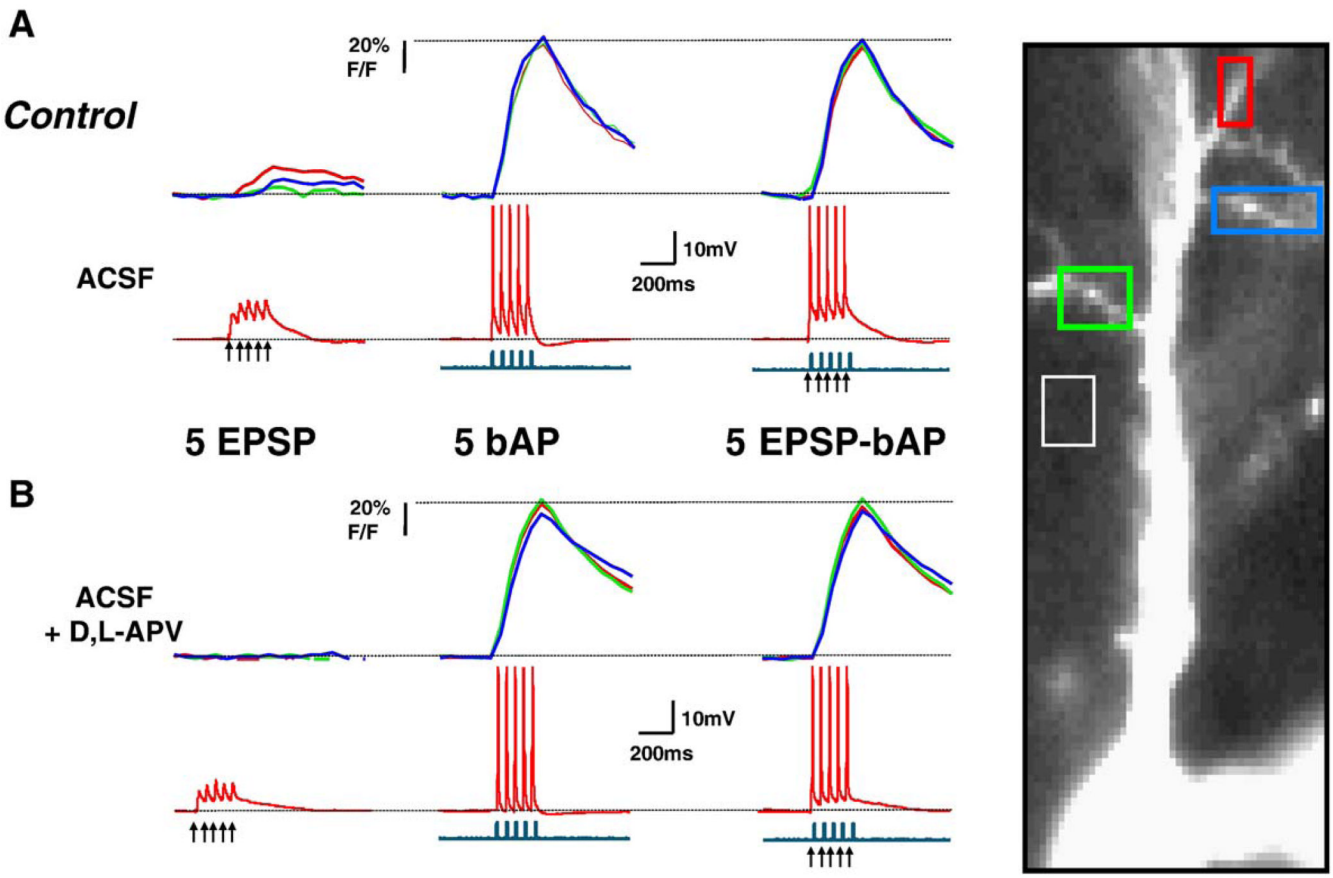

Fig. 2.

Dendritic Ca^{2+} changes evoked by coincident EPSPs-bAPs in control neurons are of similar amplitude to those evoked by bAPs alone. (A) Simultaneous current-clamp and Ca^{2+} imaging in a control CA1 neuron. (B) Responses after application of D, L-APV (100 μM) to the same neuron. The top traces in A and B represent the Ca^{2+} levels estimated by changes in OGB-1 fluorescence, expressed as % $\Delta F/F$, which is proportional to Ca^{2+} concentration. The middle traces are the simultaneous recordings of membrane voltage (red), and the bottom ones, of membrane current (blue); action potentials are truncated for clarity. Arrowheads mark the onset of afferent extracellular stimulation. All data are from a sequential recording from the same CA1 pyramidal neuron. The same figure scheme is used in Fig. 3. (For interpretation of the references to colour in this figure legend, the reader is referred to the web version of this article.)

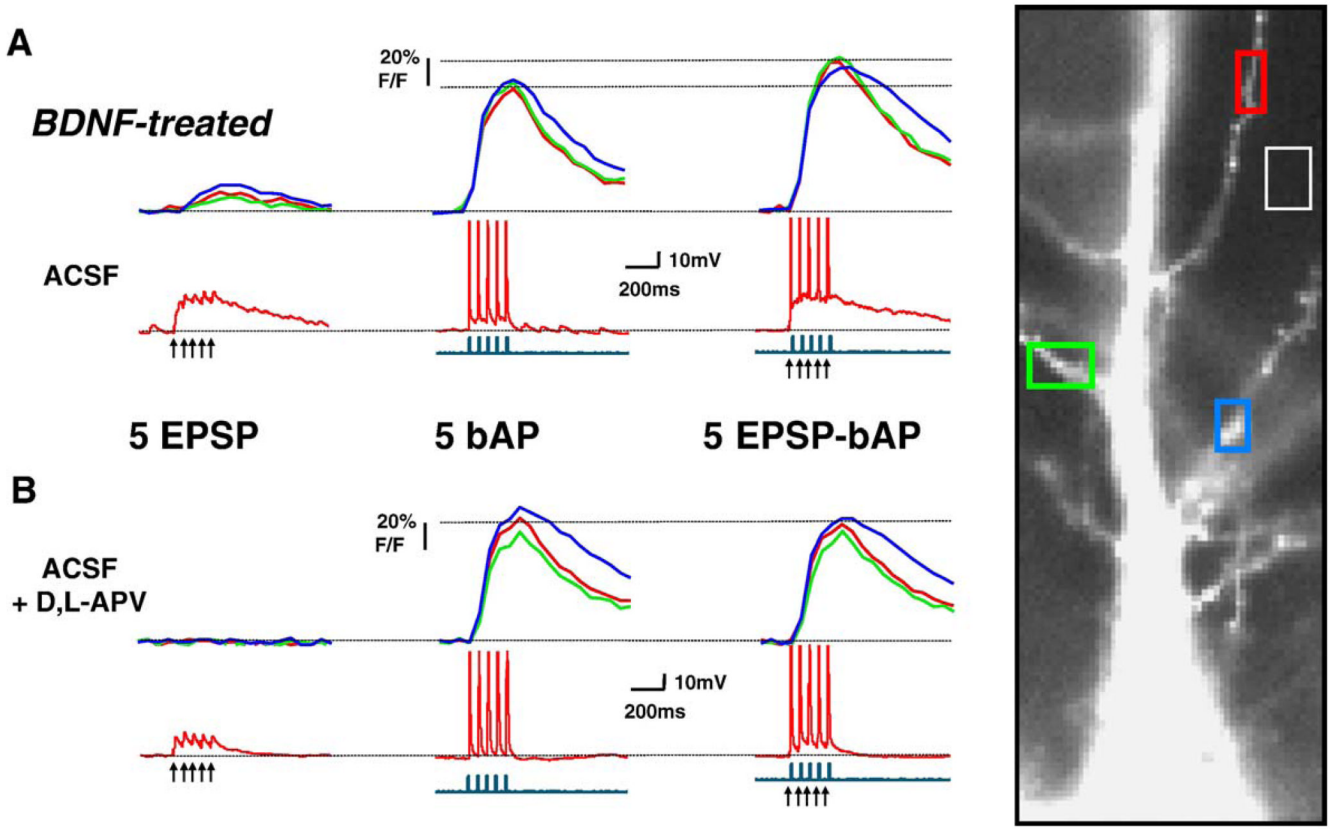

Fig. 3.

Dendritic Ca^{2+} changes evoked by coincident EPSPs-bAPs in BDNF-treated neurons are larger than those evoked by bAPs alone. The data in this figure are presented in the same way as that in Fig. 2.

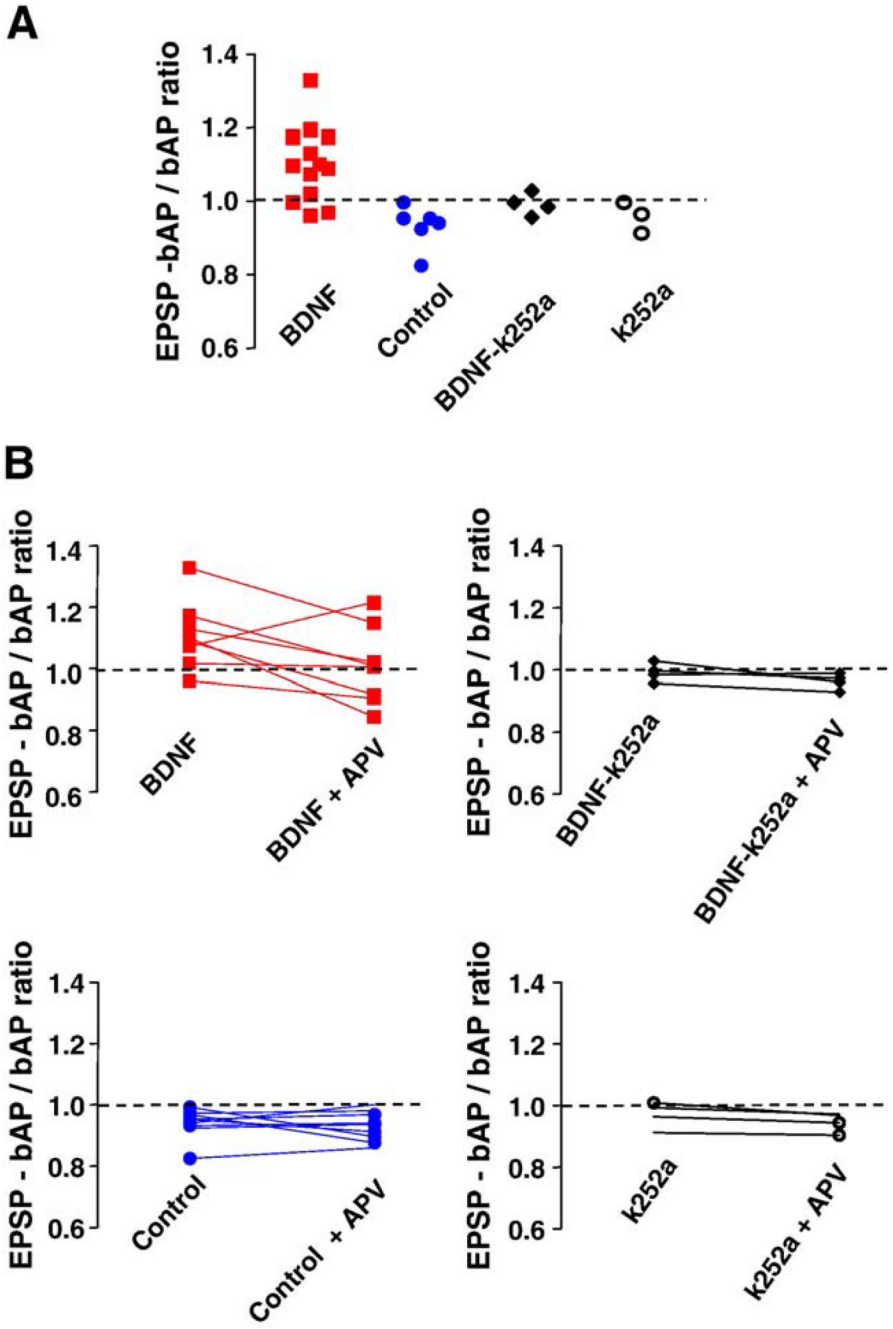

Fig. 4.

Coincident EPSP-bAP trains evoked larger dendritic Ca^{2+} signals than bAPs alone, but only in BDNF-treated neurons. (A) The ratio of dendritic Ca^{2+} signals evoked by coincident EPSP-bAP to those evoked by bAPs alone is larger than 1 in BDNF-treated neurons. This ratio was used to estimate the contribution of synaptically originated Ca^{2+}- presumably from individual spines - to Ca^{2+} signals in dendrites. Ten out of thirteen cells treated with BDNF exhibited an EPSP-bAP/bAP ratio larger than 1, whereas all 10 serum-free cells showed a less-than-1 ratio. Co-application of the receptor tyrosine kinase inhibitor k-252a prevented the effect of BDNF, without an effect of its own. (B) The ratio of the dendritic Ca^{2+} signal evoked by coincident EPSP-bAP to that evoked by bAPs alone before and after application of D, L-APV. NMDAR

blockade equalized the ratio in BDNF-treated cells, without having an effect in control neurons, or in neurons exposed to k-252a alone or in combination with BDNF. These results suggest that the activation of NMDARs during paired EPSP-bAP contributes to dendritic Ca^{2+} signals only in BDNF-treated neurons.

Table 1

Amplitude of Ca^{2+} changes evoked by subthreshold EPSPs bAPs, or SPSP bAP pairings in secondary apical dendrites of CA1 pyramidal neurons

	Control (10)	BDNF (13)	k-252a (4)	BDNF + k-252a (4)
5 EPSPs (% Δ*F*/*F*)	16.2 ± 4.1	13.8 ± 3.6	8.5 ± 1.9	9.1 ± 0.3
5 bAPs (% Δ*F*/*F*)	143 ± 8.4	125.5 ± 14.6	112 ± 11.2	121.5 ± 4.6
5 EPSP-bAP (% Δ*F*/*F*)	135.2 ± 8	140 ± 18.1	109.1 ± 12.8	120.4 ± 3.3

Data are expressed as mean ± standard error of the mean (SEM). Numbers in parenthesis denote number of cells from as many different slices.